The SH2 domain of Bcr-Abl is not required to induce a murine myeloproliferative disease; however, SH2 signaling influences disease latency and phenotype

Xiaowu Zhang, Ray Wong, Sheryl X. Hao, Warren S. Pear, and Ruibao Ren

Bcr-Abl plays a critical role in the pathogenesis of chronic myelogenous leukemia (CML). It was previously shown that expression of Bcr-Abl in bone marrow cells by retroviral transduction efficiently induces a myeloproliferative disorder (MPD) in mice resembling human CML. This in vivo experimental system allows the direct determination of the effect of specific domains of Bcr-Abl, or specific signaling pathways, on the complex in vivo pathogenesis of CML. In this report, the function of the SH2 domain of Bcr-Abl in the pathogenesis of CML is examined using this murine model. It was found that the Bcr-Abl SH2 mutants retain the ability to induce a fatal MPD but with an extended latency compared with wild type (wt) Bcr-Abl. Interestingly, in contrast to wt Bcr-Abl–induced disease, which is rapid and monophasic, the disease caused by the Bcr-Abl SH2 mutants is biphasic, consisting of an initial B-lymphocyte expansion followed by a fatal myeloid proliferation. The B-lymphoid expansion was diminished in mixing experiments with *bcr-abl*/ΔSH2 and wt *bcr-abl* cells, suggesting that the Bcr-Abl–induced MPD suppresses B-lymphoid expansion. (Blood. 2001;97:277-287)

Introduction

The *bcr-abl* oncogene is produced when the break-point cluster region gene (*c-bcr*) sequences on chromosome 22 are fused to *c-abl* sequences on chromosome 9 by a reciprocal translocation.[1] The Bcr-Abl fusion protein is present in nearly all patients with chronic myelogenous leukemia (CML) and in some patients with acute lymphoblastic leukemia. Depending on the nature of the translocation and exactly how the *bcr* and *abl* sequences become spliced into a final *bcr-abl* messenger RNA, various Bcr-Abl fusion proteins including p185, p210, and p230 can be generated, which show a preferential association with different types of leukemia.[2]

CML is a clonal myeloproliferative disorder (MPD) resulting from the neoplastic transformation of hematopoietic stem cells.[1,3] The disease usually has a biphasic course, comprising a chronic phase and a blast phase. The initial chronic phase is characterized by accumulation of large numbers of myeloid-lineage cells predominated by granulocytes in peripheral blood (PB), bone marrow (BM), and spleen. It is not clear why CML manifests as an MPD, even though Bcr-Abl is expressed in the hematopoietic stem cell compartment in humans and Bcr-Abl has the capacity to transform nearly all hematopoietic elements. Progression of the disease after 3 to 5 years to terminal blast phase, often through an accelerated phase, is characterized by accelerated accumulation of immature myeloid or lymphoid cells. Bcr-Abl is important in both initiation and maintenance of neoplastic transformation[4]; however, disease progression to blast crisis likely requires additional mutations.[1,5]

Bcr-Abl contains many domains/motifs that regulate and mediate its function. Abl-derived sequences from Bcr-Abl contain Src-homology-3 (SH3), SH2, and tyrosine kinase domains in its N-terminal half, as well as a DNA binding domain, an actin binding domain, nuclear localization signals, and SH3 binding sites in its C-terminal region.[6] The Bcr region of Bcr-Abl/p210 contains a coiled-coil oligomerization domain, a serine/threonine kinase domain, a pleckstrin homology domain, a Dbl/CDC24 guanine-nucleotide exchange factor homology domain, and several serine/threonine and tyrosine phosphorylation sites and binding sites for the Abl SH2 domain, Grb2, Grb10, and 14-3-3 proteins.[7,8] Defining the roles of these domains/motifs of Bcr-Abl is critical for understanding the molecular mechanism of Bcr-Abl leukemogenesis.

The SH2 domain is a modular unit present in a wide variety of signaling molecules.[9,10] It mediates specific protein-protein interactions by binding phosphotyrosine-containing peptides. Some SH2 domains can also bind peptides in a phosphotyrosine-independent manner and some can even bind phospholipids.[11-14] The SH2 domains of intracellular protein–tyrosine kinases play a role in the catalytic function of the kinases.[15,16] They may contribute to the kinase substrate specificity by protecting the substrates from dephosphorylation, localizing them to a specific subcellular location, or facilitating processive phosphorylation of multiple tyrosine residues in the same protein.[17] The SH2 domain plays an important role in the Abl proteins in interacting with and phosphorylating signaling proteins, including p62dok, c-Cbl, Rin-1, Tub, and mDab1.[18-24] It can also interact with Bcr sequences and Shc through phosphotyrosine-independent interactions.[11,25]

The Abl SH2 domain is required for transformation of cultured fibroblast cells by Bcr-Abl.[26] However, mutations in the Abl SH2 domain do not diminish the ability of Bcr-Abl to render cytokine-independent growth of factor-dependent hematopoietic cell lines.[27-31] In addition, Bcr-Abl SH2 mutants can transform primary lymphoid

From the Rosenstiel Basic Medical Sciences Research Center, Department of Biochemistry, and Department of Biology, Brandeis University, Waltham, MA; and Department of Pathology and Institute for Medicine and Engineering, University of Pennsylvania, Philadelphia, PA.

Submitted May 1, 2000; accepted October 5, 2000.

Supported by ACS grant RPG-97-131-01-LBC (R.R.) and NIH RO1 CA77570-01 (W.S.P.). W.S.P. and R.R. are recipients of the Leukemia and Lymphoma Society Scholar Award.

Reprints: Ruibao Ren, Rosenstiel Basic Medical Sciences Research Center, MS 029, Brandeis University, 415 South St, Waltham, MA; e-mail: ren@hydra.rose.brandeis.edu.

The publication costs of this article were defrayed in part by page charge payment. Therefore, and solely to indicate this fact, this article is hereby marked "advertisement" in accordance with 18 U.S.C. section 1734.

progenitors in vitro as well as wild-type (wt) Bcr-Abl.[28] These conflicting observations in cultured cells suggest that the requirement for the SH2 domain is cell type- or context-dependent. Attempts have also been made to assess the role of the SH2 domain in Bcr-Abl leukemogenesis in vivo. It was shown that the pre–B-lymphoid cells transformed by Bcr-Abl SH2 mutants were poorly tumorigenic in immunodeficient mice.[28] The SH2 domain of Bcr-Abl was also shown to be required for developing a myeloid leukemia in mice due to failure to activate phosphatidylinositol (PI)-3 kinase/Akt pathway.[32] However, in earlier models, Bcr-Abl does not effectively induce CML-like MPD,[33-37] making it difficult to conclude whether the SH2 domain plays a role in pathogenesis of CML.

We and others recently have shown that expression of Bcr-Abl in BM cells by retroviral transduction efficiently induces an MPD in mice resembling human CML.[38-40] This murine model for CML provides an effective in vivo experimental system to study the roles and relative importance of domains of Bcr-Abl and of signaling events affected by Bcr-Abl in leukemogenesis.[41] In this report, we used our in vivo model to study the function of Bcr-Abl SH2 domain in the pathogenesis of CML. We found that SH2 mutations slowed the onset of, but did not prevent, Bcr-Abl–induced MPD. The phenotype of the disease induced by Bcr-Abl SH2 mutants differed from wt Bcr-Abl disease in that the SH2 mutants induced a B-lymphoproliferative disorder prior to the fatal MPD. The B-cell lymphocytosis could be suppressed by wt Bcr-Abl–induced MPD in a mixing experiment, suggesting that Bcr-Abl–induced MPD suppresses B-lymphoid expansion. This may provide a clue to the specificity of MPD induction by Bcr-Abl in CML.

Materials and methods

DNA constructs

The R1057K mutation was introduced into Bcr-Abl/p210 by first amplifying 2 overlapping fragments containing this point mutation from the *bcr-abl/p210* gene[38] by polymerase chain reaction (PCR) with 5′ primer NT114: 5′-ATCACGCCAGTCAACAGTC-3′; and 3′ primer NT112: 5′-CTC TCACTCTCTTTCACCAAGAAGCTGCCATTG-3′ (containing the mutation) for fragment 1; and with 5′ primer NT113: 5′-CTTCTTGGTGAAAGAGAGTGAGAGCAGTCC-3′ (containing the mutation); and 3′ primer NT39: 5′-GGACATGCCATAGGTAGC-3′ for fragment 2. We then purified these 2 fragments with the QIAquick PCR Purification Kit (Qiagen Inc, Chatsworth, CA) and mixed them together as templates to generate fragment 3 by PCR with 5′ primer NT114 and 3′ primer NT39. Fragment 3 was then digested with restriction enzymes *Hinc*II and *Aat*II and subcloned into the corresponding position in the *bcr-abl/p210* gene to generate *bcr-abl/R1057K* complementary DNA. To generate *bcr-abl/*Δ*SH2*, we used the 5′ primer NT62: 5′-GAATTCGTCAACAGTCTGGAGCCCACTGTCTATGGTGTGTCC-3′ (corresponding to the sequences flanking both ends of the SH2 domain) and 3′ primer NT39 (see above) to amplify the ΔSH2 fragment from *bcr-abl/p210* by PCR. The ΔSH2 fragment was digested with *Hinc*II and *Aat*II and was subcloned into the corresponding position in *bcr-abl/p210* to generate *bcr-abl/*Δ*SH2* complementary DNA. Both *bcr-abl/R1057K* and *bcr-abl/*Δ*SH2* were cloned into the *Eco*RI site in MSCV-IRES-gfp (murine stem cell retroviral vector–internal ribosomal entry site–green fluorescence protein) vector as previously described.[38] The portions of *bcr-abl/R10 57K* and *bcr-abl/*Δ*SH2* that were produced by PCR amplification were verified to be correct by sequencing.

Cell culture and retrovirus preparation

NIH3T3 mouse fibroblasts were grown in Dulbecco modified Eagle medium (DMEM) containing 10% calf serum, 100 U/mL penicillin (Gibco BRL, Grand Islands, NY), and 100 μg/mL streptomycin (Gibco BRL). Helper-free retroviruses were generated by transiently transfecting retroviral constructs into BOSC 23 cells as described.[42] Two days after transfection, the culture supernatant containing the retroviruses was collected and used to transduce BM cells for the CML model and NIH3T3 cells for determination of a relative viral titer. The virus preparation can be stored at 4°C for up to 4 days without significant change in virus titer. Retroviral transduction and titering were performed as described.[38,41] All viruses were adjusted to equal titer based on GFP expression with BOSC 23–conditioned medium just before transduction of BM cells or other cell types.

BM transduction and transplantation

BM cell transduction and transplantation were performed as previously described.[38]

Flow cytometry and cell sorting

Flow cytometry and cell sorting were performed as described.[38,41]

Southern blot

PB obtained from the orbital sinus or tail and dispersed cells from spleen were treated with red blood cell lysis solution ACK (150 mM NH_4Cl, 1 mM $KHCO_3$, 0.1 mM Na_2 ethylenediaminetetraacetic acid, pH 7.3). High molecular weight DNA from the white blood cells (WBCs) and sorted splenocytes was isolated by using the QIAamp Blood Kit (Qiagen). For proviral integration analysis, up to 15 μg DNA was digested with either *Eco*RI, *Bam*HI, or *Bgl*II, separated on a 1% agarose gel, transferred to Hybond-N^+ membrane (Amersham, Arlington Heights, IL), and hybridized with a probe containing IRES-gfp sequences derived from the retroviral vector as described.[38] For determining the contribution of *bcr-abl*- and *bcr-abl/*Δ*SH2*–transduced cells in BM mixing experiments, genomic DNA from PB was digested with *Hind*III and separated on a 0.7% agarose gel, transferred to Hybond-N^+ membrane, and hybridized with a probe corresponding to a 1.2-kilobase (kb) *Eco*47III-*Bgl*II fragment of the 3′ end of human c-abl complementary DNA. The washed membrane was exposed to X-ray film.

Immunoblotting

NIH3T3 cells were transduced with titer-matched viruses as described above. Two days after transduction, cells were serum-starved with DMEM containing 0.1% calf serum for 12 hours. The cells were then collected, washed once in ice-cold phosphate-buffered-saline (PBS) (Gibco BRL), resuspended in certain volume in ice-cold PBS, and boiled for 5 minutes in an equal volume of 2 × sodium dodecyl sulfate (SDS) sample buffer as described.[43] The ACK-treated spleen cells were resuspended in ice-cold PBS at 2×10^6 cells/mL, lysed by adding equal volume of 2 × SDS sample buffer, and heated at 100°C for 5 minutes. Cell debris was cleared by centrifugation. Equal amounts of total protein of each lysate were run on 6% to 15% SDS-polyacrylamide gradient gels and transferred to nitrocellulose filters. Protein blots were probed with antibodies as described previously,[41] with the exception that the signal transducer and activator of transcription (STAT)5 antibody was purchased from Transduction Laboratories (Lexington, KY). Bound antibodies were visualized using horseradish peroxidase–conjugated antimouse or antirabbit immunoglobulin G (IgG) and enhanced chemiluminescence reagents as described by the manufacturer (Amersham).

Immunokinase assay

Retroviral constructs were transfected into BOSC 23 cells as described.[42] Two days after transfection, cells were lysed in lysis buffer (50 mM HEPES, pH7.4; 150 mM NaCl; 10% glycerol; 1% Triton X-100; 1 mM EGTA; 1.5 mM $MgCl_2$; 1 mM dithiothreitol [DTT]; 10 mM NaF; 1 mM sodium orthovanadate; 1 mM freshly made phenylmenthylsulfonyl fluoride; 1 × complete protease inhibitor cocktail [Boehringer Mannheim, Indianapolis, IN]). Cell lysates were quantified with the Coomassie Protein Assay Reagent (Pierce, Rockford, IL) and adjusted to equal concentration with the above lysis buffer. One-milligram total proteins (in 500 μL) was

immunoprecipitated with anti-Abl antibody Ab-3 as described.[43] Immunoprecipitates were washed 3 times in lysis buffer and twice in kinase buffer (10 mM $MgCl_2$, 1 mM DTT, 50 mM HEPES) and were then aliquoted equally into 3 Eppendorf tubes: 1 for Western blotting and 2 for kinase assays with substrate glutathione-S-transferase (GST)-10a and GST–Crk-II (Long and Ren, unpublished data, 1996), respectively. The p10a was isolated as a Src-SH3 binding polypeptide and subsequently was shown to be part of a signal integrating protein, Sin.[44,45] It contains 92 amino acids including a single tyrosyl residue followed by amino acids Asp-Val-Pro. We found that p10a can be phosphorylated by the Abl protein tyrosine kinase in vitro (Long and Ren, unpublished data, 1996). The kinase assay was performed in total volume of 30 μL containing 1 × kinase buffer, 1 μg substrate, 0.5 mM adenosine triphosphate (ATP), and 1.85×10^5 Bq (5 μCi) γ-[^{32}P]ATP for 30 minutes at room temperature. Kinase reactions were terminated by adding 30 μL 2 × SDS sample buffer and heating at 100°C for 10 minutes. Equal amounts of supernatant were analyzed by SDS-polyacrylamide gel electrophoresis and autoradiography.

Enzyme-linked immunosorbent assay for IL-3 and GM-CSF

PB from the orbital sinus was collected into an Eppendorf tube, incubated at room temperature for 4 hours, and then incubated at 4°C overnight. The samples were spun at 16 000 rpm in a microcentrifuge at 4°C. The supernatant was transferred into a new tube and frozen at −70°C until use. The serum levels of interleukin (IL)–3 and granulocyte-macrophage colony-stimulating factor (GM-CSF) were assayed using mouse IL-3 and GM-CSF enzyme-linked immunosorbent assay (ELISA) kit from R & D Systems (Minneapolis, MN) and Endogen (Woburn, MA), respectively.

Results

Bcr-Abl with mutations in its SH2 domain causes a transient B-lymphoproliferative disorder and a delayed MPD in mice

Two Bcr-Abl SH2 mutants were made to study the role of the SH2 domain in Bcr-Abl–mediated leukemogenesis. Bcr-Abl/R1057K is Bcr-Abl with a single arginine-to-lysine mutation (R1057K) in the conserved FLVRES motif of the SH2 domain. This mutation has been shown to significantly reduce the ability of the SH2 domain to bind tyrosine-phosphorylated proteins but does not affect the overall NMR structure of the SH2 domain.[46] Bcr-Abl/ΔSH2 is Bcr-Abl with its SH2 domain deleted. To examine the effect of the SH2 mutations on the expression of Bcr-Abl, NIH3T3 cells were transduced with titer-matched retroviruses containing wt *bcr-abl* or its SH2 mutants. Western blot analysis of the lysates of these cells showed that wt Bcr-Abl, Bcr-Abl/R1057K, and Bcr-Abl/ΔSH2 expressed at the same level in transduced NIH3T3 cells (Figure 1A).

Bcr-Abl and SH2 mutants were transiently expressed in 293T cells, and the kinase activity of the immunoprecipitated Bcr-Abl proteins were measured by an in vitro kinase assay. As shown in Figure 1B, both Bcr-Abl/R1057K and wt Bcr-Abl were equivalent in their ability to phosphorylate themselves and exogenous substrates Crk-II (Figure 1Bi, compare lanes 1 and 3) and 10a (Figure 1Bii, compare lanes 1 and 3). In contrast, deletion of the SH2 domain showed a slight decrease in the ability to phosphorylate exogenous substrates (Figure 1Bi, Bii, lane 4) and a more significant reduction in autophosphorylation of Bcr-Abl/ΔSH2 itself (Figure 1Bi, lane 4). Kinase-deficient Bcr-Abl (Figure 1B, lane 2) was used as a negative control. The low level of phosphorylation seen in this control may be due to the presence of endogenous c-Abl (Figure 1Biii).

To examine the leukemogenicity of the SH2 mutants of Bcr-Abl in vivo, we transduced 5-fluorouracil–treated mouse BM cells in vitro with titer-matched retroviruses containing wt *bcr-abl* or its SH2 mutants and transplanted these cells into lethally irradiated syngeneic recipient mice as previously described.[38] Mice transplanted with BM cells transduced with wt *bcr-abl* virus (Bcr-Abl mice) died within 3 weeks after BM transplantation (BMT) with characteristics of the CML-like syndrome previously described[38] (Figure 2). Bcr-Abl/R1057K mice and Bcr-Abl/ΔSH2 mice also developed a fatal disease but with a significantly longer latency than Bcr-Abl mice (Mantel-Cox [log-rank] test $\chi^2 = 23.97$, $P < .0001$ and $\chi^2 = 30.28$, $P < .0001$, respectively) (Figure 2). In addition, the disease latency of Bcr-Abl/ΔSH2 mice was significantly longer than that of Bcr-Abl/R1057K mice ($\chi^2 = 12.93$, $P = .0003$).

The Bcr-Abl/R1057K and Bcr-Abl/ΔSH2 mice not only survived longer than the wt Bcr-Abl mice but also showed different

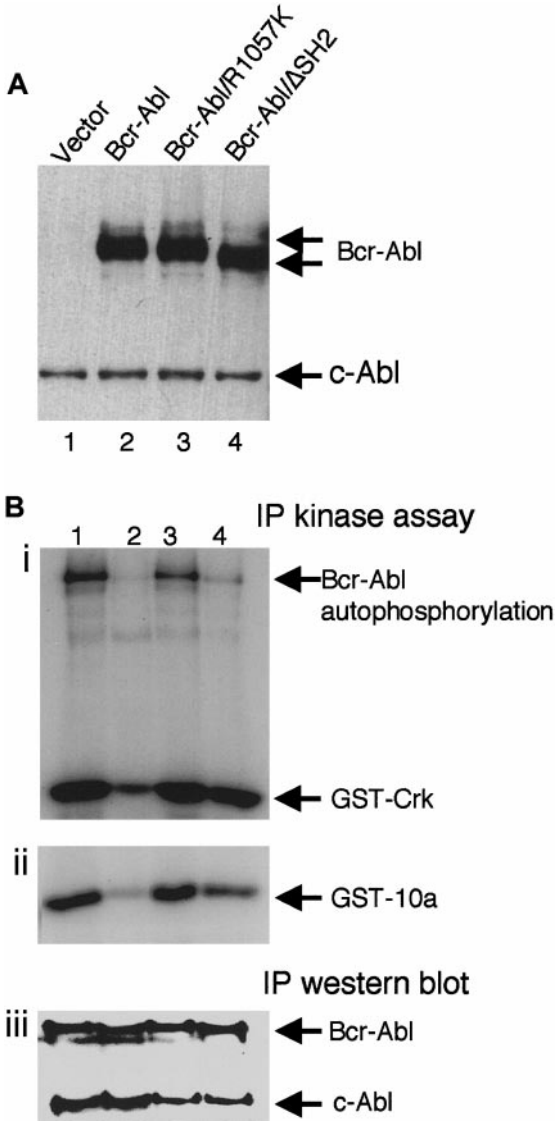

Figure 1. Expression and kinase activity of wt Bcr-Abl and the SH2 mutants. (A) Equal amounts of total lysates of NIH3T3 cells transduced with titer-matched viruses carrying *gfp* alone (lane 1), *bcr-abl* (lane 2), *bcr-abl/R1057K* (lane 3), or *bcr-abl/ΔSH2* (lane 4) were analyzed by immunoblotting with anti-Abl antibody, Ab-3. The positions of Bcr-Abl and the endogenous c-Abl are indicated. (B) Bcr-Abl (lane 1), kinase-deficient Bcr-Abl/K1176R (lane 2), Bcr-Abl/R1057K (lane 3), and Bcr-Abl/ΔSH2 (lane 4) were transiently expressed in 293T cells, immunoprecipitated with an anti-Abl antibody (Ab-3), and subjected to an in vitro kinase assay using substrate GST-Crk (i) or GST-10a (ii) as well as immunoblotting with the anti-Abl antibody (iii).

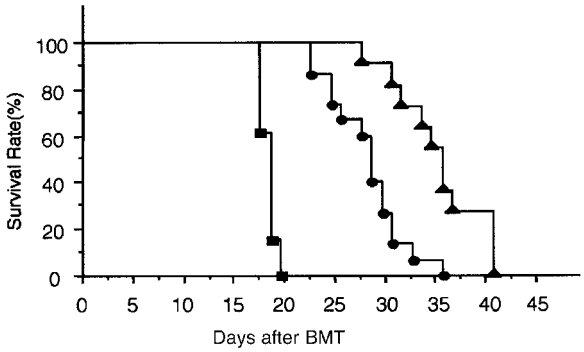

Figure 2. Survival curves of Bcr-Abl mice and SH2 mutant mice. BM cells transduced by titer-matched viruses carrying the *bcr-abl* gene or its SH2 mutants as indicated were transplanted into recipient mice. Viral constructs and number of mice used in this representative experiment: bcr-abl, ■, n = 13; bcr-abl/R1057K, ●, n = 15; bcr-abl/ΔSH2, ▲, n = 11. The survival curves were generated through Kaplan-Meier survival analysis.

hematologic manifestations. Because the pathologic consequences observed in mice receiving either Bcr-Abl/R1057K– or Bcr-Abl/ΔSH2–transduced BM cells were similar in all respects except latency, the following analysis will focus on the Bcr-Abl/ΔSH2 mice unless otherwise stated. Flow cytometric analysis showed that at day 18 after BMT, most GFP$^+$ cells in PB, spleen, and BM of wt Bcr-Abl mice were myeloid cells (Mac-1$^+$). Few B-lymphoid cells (CD19$^+$) were present (Figure 3A, Bcr-Abl). The low level of B-lymphoid cells in Bcr-Abl mice at day 18 after BMT was unlikely due to failure to reconstitute B-cell lymphopoiesis by day 18 after BMT because GFP$^+$ B-lymphoid cells were present in vector control mice at this time (Figure 3A, vector). In contrast to wt Bcr-Abl mice, there were a large number of GFP$^+$ B-lymphoid cells in the PB of Bcr-Abl/ΔSH2 mice at day 18 after BMT (Figure 3A). This difference is especially apparent in spleen and BM (compare Bcr-Abl and Bcr-Abl/ΔSH2 in Figure 3A). Most GFP$^+$ cells in the BM of wt Bcr-Abl mice were myeloid cells, whereas almost all GFP$^+$ cells in the BM of Bcr-Abl/ΔSH2 mice were B-lymphoid cells (Figure 3A) (Bcr-Abl and Bcr-Abl/ΔSH2 mice had a comparable number of cells in their BM, data not shown).

A detailed immunophenotypic analysis was performed on Bcr-Abl/ΔSH2 mice to determine the developmental stages of the B-lymphoid cells. As shown in Figure 3B, there are 78% GFP$^+$ B lymphocytes (CD19$^+$) in Bcr-Abl/ΔSH2 mouse BMT5.16 at day 27 after BMT. Among the GFP$^+$ cells, 28% cells are B220^{high}/sIgM^{high} and 66% are B220^{low}/sIgM$^{low/-}$ (Figure 3Bii). Similar results were observed in other Bcr-Abl/ΔSH2 mice. These results suggest that B-lymphoid cells in Bcr-Abl/ΔSH2 mice are at

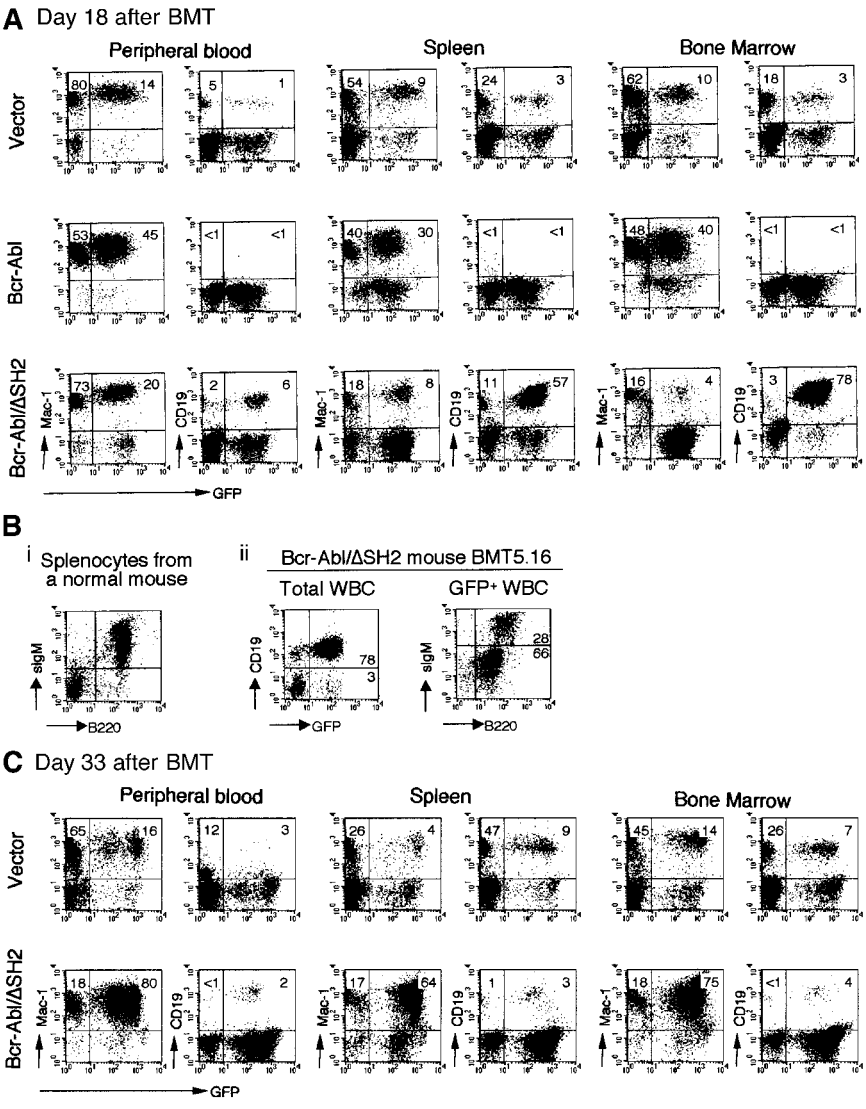

Figure 3. Immunophenotypes of the hematopoietic cells from vector, Bcr-Abl, and Bcr-Abl/ΔSH2 mice. Cells from PB, spleen, or BM were prepared and stained with the cell surface marker CD19, B220, and sIgM for B-lymphoid cells and Mac-1 for myeloid cells and analyzed on FACScaliber. (A) FACS profiles obtained from analysis of a GFP vector control mouse, BMT21.1 (top panel); a Bcr-Abl mouse, BMT21.6 (middle panel); and a Bcr-Abl/ΔSH2 mouse, BMT21.9 (bottom panel); on day 18 after BMT. (B) Expression of surface B220 and IgM on splenocytes from a normal mouse (i) and on GFP$^+$ cells from PB of Bcr-Abl/ΔSH2 mouse, BMT5.16, on day 27 after BMT (ii). (C) FACS profiles of a vector mouse, BMT21.2 (top panel); and a Bcr-Abl/ΔSH2 mouse, BMT21.10 (bottom panel); on day 33 after BMT.

different developmental stages and that Bcr-Abl/ΔSH2 interferes but does not completely block the development of B lymphocytes.

Analysis of Bcr-Abl/ΔSH2 mice at later time points showed that the B-lymphoproliferative disorder in Bcr-Abl/ΔSH2 mice was gradually replaced by a fatal MPD. As shown in Figure 3C, at day 33 after BMT, almost all GFP^+ cells were myeloid cells in PB, spleen, and BM of Bcr-Abl/ΔSH2 mice. Like wt Bcr-Abl, Bcr-Abl/ΔSH2 also induced expansion of a large population of bystander (GFP^-) myeloid cells (Figure 3A,C). This result suggests that Bcr-Abl/ΔSH2 retains the ability to stimulate proliferation of normal myeloid cells, as described previously for wt Bcr-Abl mice.[38]

To further reveal the kinetics of the expansion of myeloid and B-lymphoid cells in wt Bcr-Abl mice and Bcr-Abl/ΔSH2 mice, we quantified myeloid and B-lymphoid cells in these mice at different time points after BMT. We counted the total WBCs in PB and determined the percentages of B-lymphoid and myeloid cells by flow cytometric analysis. We then calculated the absolute number of B-lymphoid cells and myeloid cells by multiplying the total number of WBCs by the percentages of B-lymphoid and myeloid cells, respectively. As shown in Figure 4A, the total number of WBCs in wt Bcr-Abl mice was already elevated at day 14 after BMT and this number increased very quickly until the mice died shortly after. In Bcr-Abl/ΔSH2 mice, on the other hand, the total number of WBCs was low even at day 16 after BMT; it increased slowly at the early phase of disease (from day 13 to day 27 after BMT); and it then increased rapidly in the later phase. As previously described, almost all cells were myeloid cells in wt Bcr-Abl mice independent of whether they had low WBC counts (day 14 after BMT) or high WBC counts (day 17 after BMT) (Figure 4B). In contrast, Bcr-Abl/ΔSH2 mice had fewer myeloid cells even at day 20 after BMT. The number of myeloid cells in Bcr-Abl/ΔSH2 mice increased slowly at the early phase of disease (from day 20 to day 27 after BMT) and then increased rapidly in the later phase. By the time that Bcr-Abl/ΔSH2 mice developed terminal symptoms of lethargy and cachexia, the absolute number of myeloid cells in these mice was similar to that in the wt Bcr-Abl mice (Figure 4B). In addition, the fatal MPD in the Bcr-Abl/ΔSH2 mice was oligoclonal (Figure 6) and showed the same pathologic findings as the wt Bcr-Abl mice.

The average number of B-lymphoid cells in Bcr-Abl/ΔSH2 mice increased from approximately 50×10^9/L (50 000/μL) at day 20 after BMT to its peak of about 110×10^9/L (110 000/μL) at day 22 (Figure 4B), whereas very few B-lymphoid cells were present in the wt Bcr-Abl mice. However, as the number of myeloid cells steadily increased in Bcr-Abl/ΔSH2 mice, both the absolute number and relative percentage of B cells decreased. There were only about 30×10^9/L (30 000/μL) B-lymphoid cells in Bcr-Abl/ΔSH2 mice by day 30 after BMT. All of the Bcr-Abl/ΔSH2 mice subsequently developed a fatal MPD that was identical to the MPD induced by wt Bcr-Abl. Of the more than 90 Bcr-Abl/ΔSH2 mice analyzed in 7 independent experiments, only 2 mice differed in their disease characteristics. Similar to other ΔSH2 mice, these 2 mice (in the same experiment) developed transient B-lymphocytosis but died of anemia without MPD, possibly due to failure of BM reconstitution. In summary, the major differences between the Bcr-Abl/ΔSH2 and Bcr-Abl diseases were the increased survival of the Bcr-Abl/ΔSH2 mice and the biphasic nature of the Bcr-Abl/ΔSH2 disease.

Bcr-Abl–induced MPD suppresses Bcr-Abl/ΔSH2–induced B-lymphoproliferative disorder

Bcr-Abl is capable of inducing MPD and lymphoid leukemia in mice, and the disease phenotype seems to be primarily influenced by the target cells.[33,34,38-40,47-51] In our model, similar to human CML, the *bcr-abl* oncogene is targeted into multipotential hematopoietic progenitor cells that give rise to both myeloid and lymphoid cells in mice. Although *bcr-abl*$^+$ B-lymphoid cells are present in Bcr-Abl mice, expression of wt Bcr-Abl results in the exclusive expansion of myeloid cells.[38-40] It is not clear why B-lymphoid cells fail to expand either in CML patients during chronic phase or in Bcr-Abl mice. In contrast to wt Bcr-Abl, the SH2 mutants of Bcr-Abl cause a delay in development of MPD and induce a transient B-lymphoproliferative disorder prior to the fully developed MPD. This result raises the possibility that B-cell proliferation in Bcr-Abl mice may be suppressed by the Bcr-Abl–induced expansion of myeloid cells. This leads to the prediction that Bcr-Abl SH2-mutant–induced B lymphoproliferation would be suppressed by Bcr-Abl–induced myeloid tumors.

To test this possibility, we transduced BM cells with titer-matched *bcr-abl* virus and *bcr-abl/ΔSH2* virus separately and then mixed these transduced BM cells and/or mock-transduced marrow cells at different ratios (Figure 5A) and transplanted a total of 500 000 cells into each lethally irradiated recipient mouse. As we have shown previously, up to one-tenth dilution of *bcr-abl*–transduced BM cells in mock-transduced BM does not change disease

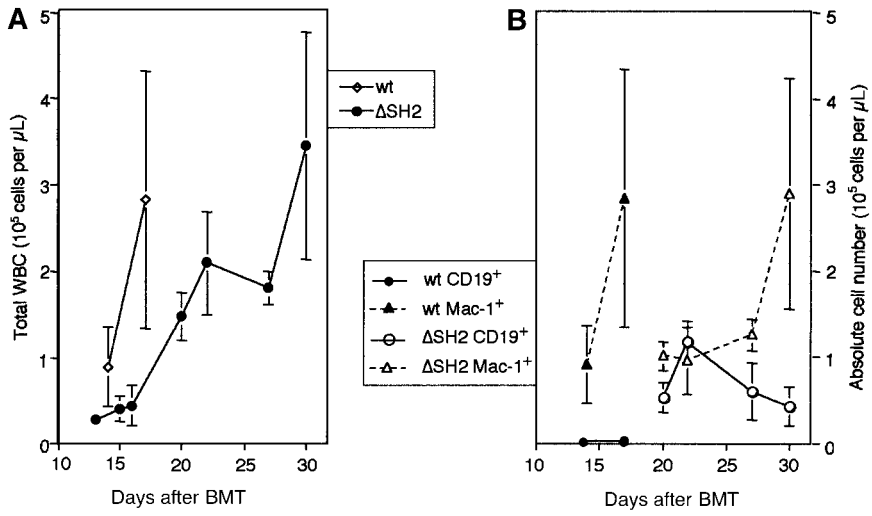

Figure 4. Expansion of myeloid and B-lymphoid cells in Bcr-Abl versus Bcr-Abl/ΔSH2 mice. The average numbers of total WBCs (A) and B-lymphoid and myeloid cells (B) in 4 Bcr-Abl versus 8 Bcr-Abl/ΔSH2 mice at different days after BMT were plotted. SDs are shown as error bars.

A

The cell composition for bone marrow mixing experiment

Recipient BMT mice	bcr-abl BM cells (x 10^5)[a]	bcr-abl/ΔSH2 BM cells (x 10^5)[a]	mock BM cells (x 10^5)[a]	Total BM cells received (x 10^5)
Bcr-Abl	4.0	0	1.0	5.0
1:4 mix	1.0	4.0	0	5.0
1:4 control	1.0	0	4.0	5.0
1:8 mix	0.5	4.0	0.5	5.0
1:8 control	0.5	0	4.5	5.0
Bcr-Abl/ΔSH2	0	4.0	1.0	5.0

[a] bone marrow cells infected by bcr-abl, bcr-abl/ΔSH2, or no virus.

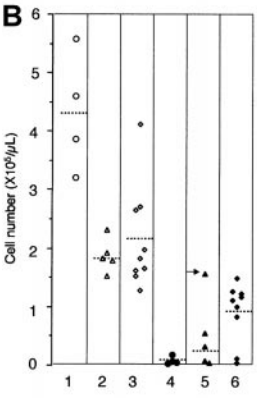

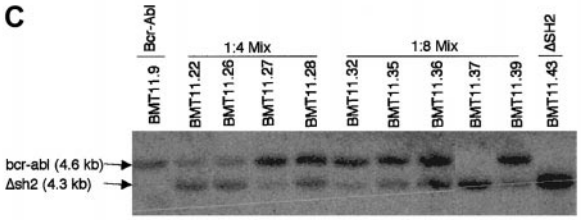

Lanes	1	2	3	4	5	6	7	8	9	10	11
bcr-abl (%)	100	27	37	82	61	77	68	63	-	67	-
Δsh2 (%)	-	73	63	18	39	23	32	37	100	33	100
Days after BMT	17	24	24	24	17	17	17	22	22	20	22
Total WBC (x10^3/μL)	424	238	348	356	192	174	273	178	232	288	166
GFP⁺ WBC (%)	49	46	47	69	39	56	35	63	69	72	75
B cells (%)	0.1	1.2	0.7	2.5	0.7	0.2	0.8	2.3	67	0.7	67
GFP⁺ B cells (%)	0	0.5	0.2	1.4	0.2	0	0.3	1.9	53	0.6	55

Figure 5. Suppression of Bcr-Abl/ΔSH2–induced B-lymphoproliferative disorder by Bcr-Abl–induced MPD. (A) Lethally irradiated recipient mice were transplanted with a mixture of mock-transduced, *bcr-abl*–transduced, and *bcr-abl/ΔSH2*–transduced BM cells at the ratio as indicated. (B) WBCs were shown for 4 1:4 mix BMT mice (column 1), 5 1:8 mix BMT mice (column 2), and 9 Bcr-Abl/ΔSH2 BMT (column 3) on day 22 after BMT. The total numbers of B-lymphoid cells ($CD19^+$) in 1:4 mix BMT mice (column 4), 1:8 mix BMT mice (column 5), and Bcr-Abl/ΔSH2 mice (column 6) are calculated as in Figure 4. (C) Genomic DNAs of PB cells from Bcr-Abl mouse (lane 1), 1:4 mix BMT mice (lanes 2-5), 1:8 mix BMT mice (lanes 6-10), and Bcr-Abl/ΔSH2 mouse (lane 11) were digested with restriction enzyme *Hind*III and subjected to Southern blot analysis with a ^{32}P-labeled 1.2-kb *Eco*47III-*Bgl*II fragment from 3′ end of human *c-abl* gene. Sizes of DNA fragments from the *bcr-abl* (4.6 kb) and *bcr-abl/ΔSH2* (4.3 kb) genes are labeled. The percentage of *bcr-abl* and *bcr-abl/ΔSH2* cells (represented by the intensity of *bcr-abl* and *bcr-abl/ΔSH2* bands) in total infected cells (represented by the sum of intensity of *bcr-abl* and *bcr-abl/ΔSH2* bands) are shown. Also shown are the total WBC counts and the percentages of GFP^+ WBC, B cells, and GFP^+ B cells in PB at the time when the DNA was made. The percentage values above 10% were shown as integers; values below 10% were rounded to the first decimal.

phenotypes except for delaying disease onset. Adding 100 000 mock-transduced BM cells to Bcr-Abl/ΔSH2 BM cells did not change the disease phenotypes of Bcr-Abl/ΔSH2 mice (data not shown).

At day 22 after BMT, Bcr-Abl/ΔSH2 mice had an average of 100×10^9/L (100 000/μL) B-lymphoid cells in PB (or 47.7% of WBCs were B cells) (Figure 5B, column 6). However, in a 1:8 (Bcr-Abl:Bcr-Abl/ΔSH2) mix, recipient mice had only 24.6×10^9/L (24 600/μL) B-lymphoid cells on average (column 5) (except for the mouse [BMT11.37] indicated by an arrow, in which only *bcr-abl/ΔSH2*$^+$ cells expanded, see below), and 1:4 mix BMT mice had only 8.9×10^9/L (8900/μL) B-lymphoid cells (column 4), even though all of these mice were transplanted with the same number of *bcr-abl/ΔSH2*–transduced BM cells. The ratio of GFP^+ B cells to GFP^- B cells did not differ significantly among Bcr-Abl/ΔSH2 mice, 1:4 mix mice, and 1:8 mix mice. Furthermore, 1:4 mix BMT mice had much higher total WBC counts (Figure 5B, column 1) than both the 1:8 mix (Figure 5B, column 2) and Bcr-Abl/ΔSH2 alone mice (Figure 5B, column 3), implying that most WBCs of 1:4 mix BMT mice at this time (day 22 after BMT) were contributed by wt Bcr-Abl–transduced myeloid cells.

There are 2 possibilities that can account for fewer B-lymphoid cells in the 1:4 mix and 1:8 mix BMT mice. One is that the expansion of myeloid cells suppresses or competes with the expansion of B-lymphoid cells as suggested above. Alternatively, Bcr-Abl–induced disease suppresses establishment of Bcr-Abl/ΔSH2–induced disease.

To distinguish between these possibilities, we investigated the relative amounts of *bcr-abl*–transduced and *bcr-abl/ΔSH2*–transduced cells in the mix BMT mice. Because *bcr-abl/ΔSH2* is 300 base pairs shorter than *bcr-abl*, it is possible to quantify the numbers of cells transduced with the 2 constructs through Southern blot analysis. Genomic DNA from PB of various diseased mice was digested with restriction enzyme *Hind*III to release a 4.6-kb DNA fragment from *bcr-abl* provirus and a 4.3-kb DNA fragment from *bcr-abl/ΔSH2* provirus. The digested genomic DNA was then analyzed by Southern blot with a *bcr-abl* DNA probe.

As shown in Figure 5C, only the upper band (4.6 kb) is detected in DNA from a Bcr-Abl mouse (Figure 5C, lane 1) and only the lower band (4.3 kb) in DNA from a Bcr-Abl/ΔSH2 mouse (Figure 5C, lane 11). Almost all 1:4 mix BMT mice (Figure 5C, lanes 2-5) and 1:8 mix BMT mice (Figure 5C, lanes 6-10) (except BMT11.37; Figure 5C, lane 9; see below) had both upper and lower bands. Quantification of the upper and lower bands indicated that both *bcr-abl* and *bcr-abl/ΔSH2* cells were expanded at comparable levels in most of the mix BMT mice (Figure 5C, *bcr-abl* [%] and *Δsh2* [%]). Although *bcr-abl/ΔSH2* cells were expanded considerably in all mix BMT mice, all mix BMT mice had very low percentages of B cells (both GFP^+ and GFP^-) in their PB compared with Bcr-Abl/ΔSH2 mice (Figure 5C). Furthermore, the absolute number of GFP^+ B cells was also much lower than expected based on the number of *bcr-abl/ΔSH2* cells in the mix BMT mice. For example, at day 20 after BMT, mouse BMT11.39 had a WBC count of 288×10^9/L (288 000/μL), of which 72% were GFP^+, and 33% of these GFP^+ (determined by Southern blot, Figure 5C), or 68.4×10^9/L (288×10^9/L × 72% × 33%) were from *bcr-abl/ΔSH2*–transduced cells. At the same day, in Bcr-Abl/ΔSH2 mice an average of 30.3% *bcr-abl/ΔSH2*–transduced (GFP^+) cells were B-lymphoid cells (GFP^+CD19^+). So, BMT11.39 was expected to have 20.73×10^9/L (68.4×10^9/L × 30.3%) GFP^+ B-lymphoid cells, but instead it had only 0.6%, or 1.73×10^9/L (288×10^9/L × 0.6%) GFP^+ B-lymphoid cells in PB (Figure 5C)—a nearly 12-fold difference between the expectation and observation. As mentioned previously, there was one 1:8 mix BMT mouse with a very high number of B-lymphoid cells (Figure 5B, column 5, arrow). This particular mouse (BMT11.37) lacked detectable wt *bcr-abl*-cells (Figure 5C, lane 9). Taken together, the results presented here strongly suggest that Bcr-Abl–induced

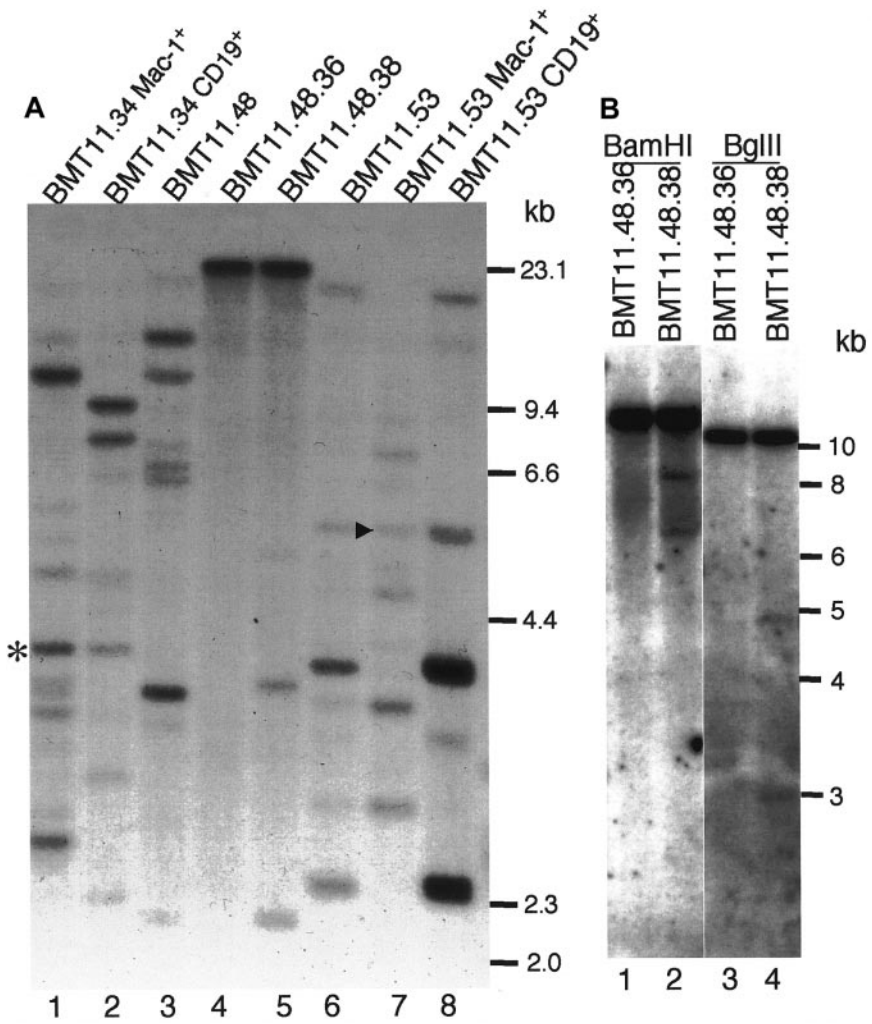

Figure 6. Proviral integration in myeloid and B-lymphoid cells from Bcr-Abl/ΔSH2 mice. (A) Genomic DNAs of PB cells of mouse BMT11.48 (lane 3) and its secondary recipients BMT11.48.36 (lane 4) and BMT11.48.38 (lane 5), sorted myeloid (lane 1) and B-lymphoid (lane 2) cells of Bcr-Abl/ΔSH2 mouse BMT11.34, and sorted myeloid (lane 7) and B-lymphoid (lane 8) cells of Bcr-Abl/ΔSH2 mouse BMT11.53 were digested with restriction enzyme *Eco*RI and analyzed by Southern blotting with ^{32}P-labeled IRES-gfp sequences. Common bands (same size) in B-lymphoid cells and myeloid cells from the same mouse are labeled with an asterisk (lanes 1,2) for BMT11.34 and an arrowhead (lanes 7,8) for BMT11.53. Sizes of *Hind*III-digested λ DNA fragments were used as DNA molecular weight markers and are shown on the right. (B) DNA from mice BMT11.48.36 and BMT11.48.38 were digested with *Bam*HI (lanes 1,2) and *Bgl*II (lanes 3,4) and analyzed by Southern blot with the same probe as in panel A. Standard 1-kb size marker is shown partially on the right.

myeloproliferative disease suppresses the Bcr-Abl/ΔSH2–stimulated proliferation of B-lymphoid cells.

The same *bcr-abl/ΔSH2*–targeted progenitor cells can give rise to both myeloid and B-lymphoid cells

Human CML is a hematopoietic stem cell disease. As described above, Bcr-Abl/ΔSH2 induces both B-lymphoproliferative disorder and MPD in mice. We wondered whether the Bcr-Abl/ΔSH2 myeloid and lymphoid cells originated from the same progenitor cells. To address this question, we purified GFP$^+$CD19$^+$ cells and GFP$^+$Mac-1$^+$ cells from the same Bcr-Abl/ΔSH2 mice by FACSorter. We then checked the proviral integration pattern in these cells by Southern blot analysis after digestion with restriction enzyme *Eco*RI (Figure 6A). Like wt Bcr-Abl mice,[38] multiple clones were expanded in primary Bcr-Abl/ΔSH2 mice (multiple bands with different intensities) (Figure 6A, lanes 3,6). Among the multiple clones from mouse BMT11.53, some were contributed only by B-lymphoid cells (Figure 6A, compare lanes 6 and 8), and some were contributed only by myeloid cells (Figure 6A, compare lanes 6 and 7). However, there was a common band in both B-lymphoid and myeloid cells (Figure 6A, arrowhead). A common band was also found in myeloid cells and B-lymphoid cells in Bcr-Abl/ΔSH2 mouse BMT11.34 (Figure 6A; lanes 1,2; asterisk). These results suggest that *bcr-abl/ΔSH2* virus can be targeted into multipotential hematopoietic progenitor cells that give rise to both myeloid and B-lymphoid cells.

We also found that the Bcr-Abl/ΔSH2–induced disease can be transferred to secondary recipient animals. In one experiment, BM cells isolated from the Bcr-Abl/ΔSH2 BMT primary mouse BMT11.48 at day 28 after BMT (its WBC counts were 126×10^9/L [126 000/μL], among which 52.6% were myeloid cells and 44.6% were B cells) were transferred into 5 secondary recipients. Among these 5 recipients, mice BMT11.48.36, BMT11.48.38, and BMT11.48.39 developed diseases. Flow cytometry analysis at day35 after BMT revealed that in secondary recipient mouse BMT11.48.36, 83% of total WBCs were GFP$^+$ myeloid cells, and there were very few (<1%) GFP$^+$ B-lymphoid cells. On the other hand, in mouse BMT11.48.38, 82% of total WBCs were GFP$^+$ B-lymphoid cells and only 1% were GFP$^+$ myeloid cells. Two days later (day 37, blood smears looked the same as on day 35, data not shown), genomic DNA was isolated from PB cells of BMT11.48.36 and BMT11.48.38. The proviral integration patterns in these mice and their parental mouse BMT11.48 were examined by Southern blot analysis (Figure 6A, lanes 3-5). Primary mouse BMT11.48 had more than 6 bands (Figure 6A, lane 3), and secondary mouse BMT11.48.36 had only 1 band (Figure 6A, lane 4), whose source must be myeloid cells. In BMT11.48.38, there was one major band, which must be largely contributed by B-lymphoid cells, and 2 minor bands (Figure 6A, lane 5). The major band in both BMT11.48.36 and BMT11.48.38 was at the same size, suggesting that the myeloid tumor cells in BMT11.48.36 and B-lymphoid tumor cells in BMT11.48.38 originated from the same progenitor

Table 1. Serum level of IL-3 and GM-CSF in mice

Mouse group	Mice, no.	IL-3 (pg/mL)*	GM-CSF (pg/mL)*
Normal/vector control	8 (6/2)†	< 2.5‡	< 5§
Bcr-Abl/p210	3	7.8 ± 2.4	24.7 ± 9.6
R1057K/p210	6	5.2 ± 2.7 (0.107)‖	22.5 ± 9.4 (0.378)‖
ΔSH2/p210	12	7.6 ± 5.2 (0.473)‖	17.5 ± 7.8 (0.096)‖
WBC containing < 18% B cells	5	8.8 ± 8.0	23.4 ± 4.0
WBC containing ≥ 18% B cells	7	6.8 ± 2.2 (0.302)¶	13.3 ± 7.2 (0.006)¶

*Results shown as average ± SD.
†Six age-matched normal mice and 2 vector control mice.
‡Sensitivity of IL-3 ELISA kit was less than 2.5 pg/mL IL-3.
§Sensitivity of GM-CSF ELISA kit was less than 5 pg/mL GM-CSF.
‖The possibility value of Student *t* test comparing with wild-type Bcr-Abl mice.
¶The possibility value of Student *t* test between the 2 groups within ΔSH2 mice.

cell. This was confirmed by digestion with additional restriction enzymes shown in Figure 6B. The major bands in both mice BMT11.48.36 and BMT11.48.38 were at the same size upon digestion with either *Bam*HI (Figure 6B, lanes 1,2) or *Bgl*II (Figure 6B, lanes 3,4). These results support the conclusion that *bcr-abl/ΔSH2* virus was targeted into multipotential hematopoietic progenitor cells that can give rise to both myeloid and B-lymphoid cells.

Bcr-Abl SH2 mutants retain the ability to induce overproduction of IL-3 and GM-CSF in mice

We have previously found that in mice with Bcr-Abl–induced myeloproliferative disease, the *bcr-abl* virus–infected cells expressed excess IL-3 and GM-CSF.[38] This finding is consistent with the reports that Bcr-Abl can induce production of IL-3 and GM-CSF in human and mouse myeloid cell lines[52-54] and that serum levels of GM-CSF in CML patients and gene expression of IL-3 in primitive CML progenitor cells are often increased.[55-58] It is possible that overproduction of hematopoietic growth factors contributes to the neoplastic expansion of myeloid cells in CML. It has been reported that the Abl SH2 domain was required for Bcr-Abl–induced IL-3 production in FDCP-1 myeloid cell line.[54] It is therefore possible that lack of the ability of induction of IL-3 and/or GM-CSF in Bcr-Abl SH2 mutants may be responsible for their changed disease latency and phenotype. To test this possibility, we examined the production of IL-3 and GM-CSF in Bcr-Abl SH2 mutant mice, compared with wt Bcr-Abl mice and vector control mice, at different disease developmental stages. Consistent with our previous results, wt Bcr-Abl induced overproduction of IL-3 and GM-CSF in mice (Table 1). Interestingly, we detected a similar amount of IL-3 and GM-CSF in either Bcr-Abl/R1057K or Bcr-Abl/ΔSH2 mice as in Bcr-Abl mice (Table 1). This result demonstrated that the SH2 domain of Bcr-Abl is not required to induce overproduction of IL-3 and GM-CSF in vivo.

As we showed earlier, Bcr-Abl SH2 mutants induced an initial B lymphoproliferation followed by a fatal myeloproliferation. We wondered whether there were different amounts of IL-3 and GM-CSF induced at different disease development stages. Among the 12 ΔSH2 mice shown in Table 1, 7 had more than 18% (18%-64.2%) GFP^+ B-lymphoid ($CD19^+$) cells in their PB and 5 others had much less (0.14%-9.0%) GFP^+ B-lymphoid cells at the time when the serum was collected. As shown in Table 1, there is no significant difference in IL-3 level between these 2 groups ($P = .302$). Both groups of mice also overproduced GM-CSF, although mice with less GFP^+ B-lymphoid cells and more myeloid cells produced a significantly higher amount of GM-CSF ($P = .006$). The latter result suggests that the myeloid cells may be the major source of GM-CSF.

It was shown that the SH2 domain of Bcr-Abl was required both for activation of Akt and cellular transformation.[32] To test whether the differences in the disease phenotype of Bcr-Abl SH2 mutants versus wt Bcr-Abl are due to their ability to activate Akt, we examined the activation of Akt in diseased mice using an antibody that recognizes the activation-specific phosphorylated site of the protein. Figure 7A shows that Akt is expressed and phosphorylated at a similar level in hematopoietic cells isolated from wt Bcr-Abl, Bcr-Abl SH2 mutant, and vector mice. Similar results were also seen in serum-starved NIH3T3 cells containing wt Bcr-Abl, Bcr-Abl SH2 mutants, or vector alone (Figure 7B). Because Akt is activated in vector control mice and NIH3T3 cells, it is not clear whether Akt can be activated by Bcr-Abl SH2 mutants in these cells, but our results suggest that the changed disease phenotype of Bcr-Abl SH2 mutants may not be due to the ability of the mutants to activate Akt.

Activation of Ras and STAT5 has also been shown to be important for Bcr-Abl transformation.[1] We went on to examine the activation of extracellular signal-regulated kinase (Erk)1/2, a major downstream signaling protein of the Ras pathway, and STAT5 using antibodies that recognize activation-specific phosphorylated sites of these signaling proteins. Figure 7A shows that p42/Erk2 is phosphorylated in cells isolated from both wt Bcr-Abl and Bcr-Abl

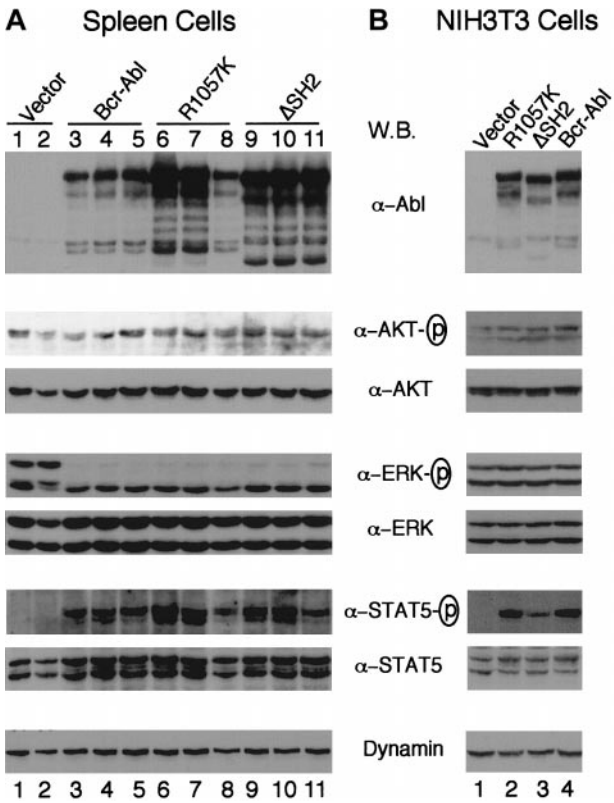

Figure 7. Expression of Bcr-Abl proteins and activation of Akt, Erk, and STAT5 in vivo and in vitro. Western blot analyses of spleen cell lysates from 2 vector mice (lanes 1,2), 3 wt Bcr-Abl mice (lanes 3-5), 3 Bcr-Abl/R1057K mice (lanes 6-8), and 3 Bcr-Abl/ΔSH2 mice (lanes 9-11) (A) and of lysates of NIH3T3 cells transduced with titer-matched viruses carrying vector alone (lane 1), *bcr-abl/R1057K* (lane 2), *bcr-abl/ΔSH2* (lane 3), or wt *bcr-abl* (lane 4) (B). The NIH3T3 cells were serum-starved for 12 hours 2 days after transduction. Equal amounts of total lysates of either spleen cells or NIH3T3 cells were separated on 6% to 15% polyacrylamide gradient gels, transferred to nitrocellulose filters, and probed with antibodies as indicated. The fresh filters were first probed with an anti-Abl antibody (Ab-3) or the phospho-specific antibodies against activated Akt, Erk, and STAT5 and then stripped and reprobed with an anti-Dynamin antibody or antibodies against corresponding Akt, Erk, and STAT5 proteins, respectively.

SH2 mutant mice. Both p44/Erk1 and p42/Erk2 were activated in cells isolated from vector control mice (Figure 7B, lanes 1,2). Both p44/Erk1 and p42/Erk2 were also activated in NIH3T3 cells containing wt Bcr-Abl, Bcr-Abl SH2 mutants, or vector alone (Figure 7B). It is not clear why p44/Erk1 was not activated in cells isolated from diseased Bcr-Abl mice.

Activation of STAT5 was detected in total spleen cells from both wt Bcr-Abl and Bcr-Abl SH2 mutant mice but not in spleen cells from the vector control mice (Figure 7A), confirming that Bcr-Abl proteins can induce STAT5 activation directly or indirectly (ie, through induced cytokine signaling) or both. To evaluate the ability of Bcr-Abl SH2 mutants to activate STAT5 directly, we measured the amount of activated phospho-STAT5 in NIH3T3 cells infected with wt Bcr-Abl, Bcr-Abl/R1057K, Bcr-Abl/ΔSH2, and vector alone (Figure 7B). STAT5 was not activated in vector control NIH3T3 cells serum-starved for 12 hours but was activated in Bcr-Abl–expressing NIH3T3 cells under the same condition (Figure 7B). Interestingly, Bcr-Abl/ΔSH2 had a greatly reduced (approximately 3-fold reduction) ability to activate STAT5 compared with wt Bcr-Abl (Figure 7B). However Bcr-Abl/R1057K retained the same STAT5 activation capability as wt Bcr-Abl. Because both Bcr-Abl/R1057K and Bcr-Abl/ΔSH2 caused a similar disease in mice, the changed disease phenotype of Bcr-Abl SH2 mutants may not be due to the ability of the mutants to activate STAT5.

Discussion

Our results show that the SH2 domain of Bcr-Abl is not required to induce a fatal MPD. However, the signaling pathways initiated by the SH2 domain of Bcr-Abl influence the disease latency and phenotype. Most strikingly, in contrast to wt Bcr-Abl–induced disease, which is rapid and monophasic, the disease caused by the Bcr-Abl SH2 mutants is biphasic, consisting of an initial B-lymphocyte expansion followed by a fatal myeloid proliferation. Although the degree of lymphocytosis is severe, it can be suppressed by Bcr-Abl–induced MPD.

The delayed expansion of myeloid cells in Bcr-Abl SH2 mutant mice is unlikely caused by the preceding B-lymphoproliferative disorder for the following 2 reasons: (1) Bcr-Abl SH2 mutants induced the outgrowth of fewer myeloid colonies from 5-fluorouracil–treated BM cells than wt Bcr-Abl in BM colony assays (data not shown); and (2) the B-lymphoproliferative disorder did not delay the MPD induced by wt Bcr-Abl; instead it was suppressed by Bcr-Abl–induced MPD in BM mixing experiments (Figure 5). These observations indicate that Bcr-Abl SH2 mutants have a diminished ability to stimulate myeloid proliferation.

The mechanism underlying the differences in the diseases caused by the SH2 mutants and wt Bcr-Abl is not completely understood. It appears unlikely to be caused by differences in tyrosine kinase activity or differences in retroviral titer. In support of the former, both the SH2 point mutant and deletion mutant cause nearly identical clinical diseases in mice. Despite the in vitro kinase activity being lower in the deletion mutant, the activity in the point mutant is similar to wt Bcr-Abl (Figure 1). The lower kinase activity in the deletion mutant may only account for a further delay of disease onset in Bcr-Abl/ΔSH2 mice compared with Bcr-Abl/R1057K mice (Figure 2). In support of the latter, we have previously shown that even though 10-fold dilution in retroviral supernatant slowed the onset of MPD from 3 weeks to 5 weeks, these mice did not develop the B-lymphocytosis observed in the Bcr-Abl SH2 mutant mice.[38] These results support the notion that specific SH2-generated signals, rather than the overall Abl kinase activity, account for the differences in disease phenotypes.

It has been reported that the Abl SH2 domain was required for Bcr-Abl–induced IL-3 production in the FDCP-1 myeloid cell line.[54] However, we detected similar levels of IL-3 and GM-CSF in serum of both Bcr-Abl and Bcr-Abl SH2 mutant mice (Table 1). We also found that Bcr-Abl SH2 mutants induced expansion of a large population of bystander (GFP^-) myeloid cells (Figure 3A,C), suggesting that Bcr-Abl/ΔSH2 retains the ability to stimulate proliferation of normal myeloid cells, as described previously for wt Bcr-Abl mice.[38] The difference in the ability of Bcr-Abl SH2 mutants to induce cytokine production in vivo versus in the FDCP-1 myeloid cell line may be due to a different cellular context or to different environment—eg, growth factor signaling in an in vivo environment may complement some of the defects of the SH2 mutation. Nevertheless, our results indicate that the changed disease latency and phenotype in Bcr-Abl SH2 mutant mice is not due to an altered production of IL-3 and GM-CSF, although we could not exclude the possibilities that Bcr-Abl may induce production of other cytokines and that the SH2 domain of Bcr-Abl may be important for production of those cytokines.

The SH2 domain of Bcr-Abl has been shown to play an important role in interacting with and regulating phosphorylation of signaling proteins, including p62dok, c-Cbl, Rin-1, and Shc.[18-22,25] The SH2 mutations abrogate the ability of Bcr-Abl to either interact or phosphorylate these proteins, which may affect multiple downstream signaling pathways. Of particular interest, the SH2 domain of Bcr-Abl has been shown to be required both for activation of the PI-3 kinase/Akt pathway and cellular transformation.[32] However, we found that Akt was activated in Bcr-Abl SH2 mutant cells in mice (Figure 7A). Although we do not know whether Akt was activated by Bcr-Abl SH2 mutants or by growth factor signaling within mice or by both, the ability of Bcr-Abl SH2 mutants to activate Akt appears not to account for the changed disease latency and phenotype in Bcr-Abl SH2 mutant mice. Similarly, there was no significant difference in Erk activation in cells isolated from both wt Bcr-Abl and Bcr-Abl SH2 mutant mice (Figure 7A). In contrast to the aforementioned signaling pathways, Bcr-Abl/ΔSH2 showed a significantly reduced ability to activate STAT5 in NIH3T3 cells (Figure 7B). However, the ability of Bcr-Abl/R1057K to activate STAT5 is similar to wt Bcr-Abl (Figure 7). Because the pathologic consequences observed in mice receiving either Bcr-Abl/R1057K– or Bcr-Abl/ΔSH2–transduced BM cells were similar in all respects except latency, reduced activation of STAT5 may not account for the phenotypic changes of the Bcr-Abl SH2 mutants. The reduced ability of Bcr-Abl/ΔSH2 in activating STAT5 may be due to its reduced kinase activity and may account for the further delay of disease onset compared with Bcr-Abl/R1057K. Consistent with the latter notion, STAT5 has been shown to regulate proliferation, differentiation, and apoptosis in hematopoietic cells[59] and to play a critical role in myelopoiesis and erythropoiesis in non–steady-state conditions, such as during the rapid expansion of cells under stress/pathologic conditions or during embryonic development.[60,61] In addition, it was found that dominant-negative STAT5 inhibits the growth of the K562 and 32Dcl3 cells.[62-64]

CML is a clonal multilineage MPD. Although hypercellularity occurs in multiple lineages such as Ph^+ erythroid and B-lymphoid cells, granulocytosis is predominant in CML patients. A similar phenomenon is observed in the murine model for CML.[38-40] It is not clear why the disease is manifested as an MPD, even though

Bcr-Abl is expressed in the hematopoietic stem cell compartment in humans and Bcr-Abl has the capacity to transform nearly all hematopoietic elements. Our findings that SH2 mutants of Bcr-Abl induced a transient B-lymphoproliferative disorder prior to a delayed MPD and that the lymphocytosis can be suppressed by Bcr-Abl–induced MPD (Figures 4,5) indicate that the Bcr-Abl–induced MPD suppresses lymphoid expansion. Suppression of the B-lymphoid expansion by the rapidly occurring MPD may be one of the mechanisms that account for the lack of B-lymphoproliferative disorder observed in CML patients and in Bcr-Abl mice. One possible mechanism underlying the suppression of B lymphoproliferation by Bcr-Abl–induced MPD is that myeloid cells may compete with lymphoid cells for hematopoietic space or cytokines required for proliferation of both cell types. Alternatively, Bcr-Abl may directly or indirectly induce production of inhibitors for lymphoproliferation. A similar mechanism may prevent erythroid expansion, because Bcr-Abl is capable of functionally replacing the erythropoietin receptor (EpoR) and supporting proliferation, differentiation, and maturation of fetal liver erythroid progenitors from $EpoR^{-/-}$ mice.[65] Yet, CML patients do not manifest erythrocytosis.

In several in vivo models, Bcr-Abl induces a pre-B (IgM^-) lymphoblastic leukemia.[33,34,40,47,48,50,51] In Bcr-Abl SH2 mutant mice, however, we found that many GFP^+ B-lymphoid cells were surface IgM^+ ($sIgM^+$) (Figure 3Bii), suggesting that Bcr-Abl SH2 mutants are not efficient for leukemic transformation in the presence of a concomitant MPD. It is possible that the SH2-linked signaling pathways are important for Bcr-Abl to block the development of B lymphocytes.

The TEL/PDGFβR fusion protein, generated by t(5;12)(q33; p13) translocation in a subset of chronic myelomonocytic leukemia, was also shown to induce a fatal MPD in mice.[66] An in vivo mutation analysis using the murine BM transduction/transplantation model showed that specific mutations that affect specific signaling pathways have different effects on disease phenotype.[66] Similar to Bcr-Abl SH2 mutants, mutation of the tyrosine residues essential for the binding of PI3K, Nck, Ras-GAP, SHP-2, and PLCγ in TEL/PDGFβR did not affect the phenotype of the MPD but extended the disease latency.[66] However, no documented B-lymphoproliferative disorder occurred prior to the myeloid disease. These data are also consistent with our data showing that the B-lymphoproliferative disorder induced by Bcr-Abl SH2 mutants is not simply a result of delayed MPD. It will be of interest to identify both common signaling pathways important for myeloproliferation induced by Bcr-Abl and TEL/PDGFβR and specific signaling events that lead to B lymphoproliferation in Bcr-Abl SH2 mutant mice.

Acknowledgments

We thank Ben Hentel and Jonathan Schatz for their help on flow cytometry.

References

1. Sawyers CL. Chronic myeloid leukemia. N Engl J Med. 1999;340:1330-1340.
2. Melo JV. BCR-ABL gene variants. Baillieres Clin Haematol. 1997;10:203-222.
3. Goldman JM. Chronic myeloid leukemia. Curr Opin Hematol. 1997;4:277-285.
4. Huettner CS, Zhang P, Van Etten RA, Tenen DG. Reversibility of acute B-cell leukemia induced by BCR-ABL1. Nat Genet. 2000;24:57-60.
5. Faderl S, Talpaz M, Estrov Z, O'Brien S, Kurzrock R, Kantarjian HM. The biology of chronic myeloid leukemia. N Engl J Med. 1999;341:164-172.
6. Wang JYJ. Abl tyrosine kinase in signal transduction and cell-cycle regulation. Curr Opin Genet Dev. 1993;3:35-43.
7. Raitano AB, Whang YE, Sawyers CL. Signal transduction by wild-type and leukemogenic Abl proteins. Biochim Biophys Acta. 1997;1333: F201–F216.
8. Ghaffari S, Daley GQ, Lodish HF. Growth factor independence and BCR/ABL transformation: promise and pitfalls of murine model systems and assays. Leukemia. 1999;13:1200-1206.
9. Cohen G, Ren R, Baltimore D. Modular binding domains in signal transduction proteins. Cell. 1995;80:237-248.
10. Pawson T. Protein modules and signalling networks. Nature. 1995;373:573-580.
11. Pendergast AM, Muller AJ, Havlik MH, Maru Y, Witte ON. BCR sequences essential for transformation by the *BCR-ABL* oncogene bind to the ABL SH2 regulatory domain in a non-phosphotyrosine-dependent manner. Cell. 1991;66:161-171.
12. Muller AJ, Pendergast AM, Havlik MH, Puil L, Pawson T, Witte ON. A limited set of SH2 domains binds BCR through a high-affinity phosphotyrosine-independent interaction. Mol Cell Biol. 1992;12:5087-5093.
13. Poy F, Yaffe MB, Sayos J, et al. Crystal structures of the XLP protein SAP reveal a class of SH2 domains with extended, phosphotyrosine-independent sequence recognition. Mol Cell. 1999;4:551-561.
14. Rameh LE, Chen CS, Cantley LC. Phosphatidylinositol (3,4,5)P3 interacts with SH2 domains and modulates PI 3-kinase association with tyrosine-phosphorylated proteins. Cell. 1995;83:821-830.
15. Duyster J, Baskaran R, Wang JYJ. Src homology 2 domain as a specificity determinant in the c-Abl-mediated tyrosine phosphorylation of the RNA polymerase II carboxyl-terminal repeated domain. Proc Natl Acad Sci U S A. 1995;92:1555-1559.
16. Mayer BJ, Hirai H, Sakai R. Evidence that SH2 domains promote processive phosphorylation by protein-tyrosine kinases. Curr Biol. 1995;5:296-305.
17. Pawson T. Getting down to specifics. Nature. 1995;379:477-478.
18. Yamanashi Y, Baltimore D. Identification of the Abl- and rasGAP-associated 62 kDa protein as a docking protein, Dok. Cell. 1997;88:205-211.
19. Carpino N, Wisniewski D, Strife A, et al. p62(dok): a constitutively tyrosine-phosphorylated, GAP-associated protein in chronic myelogenous leukemia progenitor cells. Cell. 1997;88:197-204.
20. Bhat A, Johnson KJ, Oda T, Corbin AS, Druker BJ. Interactions of p62(dok) with p210(bcr-abl) and Bcr-Abl-associated proteins. J Biol Chem. 1998;273:32360-32368.
21. Bhat A, Kolibaba K, Oda T, Ohno-Jones S, Heaney C, Druker BJ. Interactions of CBL with BCR-ABL and CRKL in BCR-ABL-transformed myeloid cells. J Biol Chem. 1997;272:16170-16175.
22. Afar DE, Han L, McLaughlin J, et al. Regulation of the oncogenic activity of BCR-ABL by a tightly bound substrate protein RIN1. Immunity. 1997;6: 773-782.
23. Kapeller R, Moriarty A, Strauss A, et al. Tyrosine phosphorylation of tub and its association with Src homology 2 domain-containing proteins implicate tub in intracellular signaling by insulin. J Biol Chem. 1999;274:24980-24986.
24. Howell BW, Gertler FB, Cooper JA. Mouse disabled (mDab1): a Src binding protein implicated in neuronal development. EMBO J. 1997;16:121-132.
25. Raffel GD, Parmar K, Rosenberg N. In vivo association of v-Abl with Shc mediated by a non-phosphotyrosine-dependent SH2 interaction. J Biol Chem. 1996;271:4640-4645.
26. Afar DEH, Goga A, McLaughlin J, Witte ON, Sawyers CL. Differential complementation of Bcr-Abl point mutants with c-Myc. Science. 1994;264: 424-426.
27. McWhirter JR, Wang JYJ. An actin-binding function contributes to transformation by the Bcr-Abl oncoprotein of Philadelphia chromosome-positive human leukemias. EMBO J. 1993;12:1533-1546.
28. Goga A, McLaughlin J, Afar DE, Saffran DC, Witte ON. Alternative signals to RAS for hematopoietic transformation by the Bcr-Abl oncogene. Cell. 1995;82:981-988.
29. Cortez D, Kadlec L, Pendergast AM. Structural and signaling requirments for Bcr-Abl-mediated transformation and inhibition of apoptosis. Mol Cell Biol. 1995;15:5531-5541.
30. Oda T, Tamura S, Matsuguchi T, Griffin JD, Druker BJ. The SH2 domain of Abl is not required for factor-independent growth induced by Bcr-Abl in a murine myeloid cell line. Leukemia. 1995;9: 295-301.
31. Ilaria RL Jr, Van Etten RA. The SH2 domain of P210BCR/ABL is not required for the transformation of hematopoietic factor-dependent cells. Blood. 1995;86:3897-3904.
32. Skorski T, Bellacosa A, Nieborowska-Skorska M, et al. Transformation of hematopoietic cells by BCR/ABL requires activation of a PI-3k/Akt-dependent pathway. EMBO J. 1997;16:6151-6161.
33. Daley GQ, Van Etten RA, Baltimore D. Induction of chronic myelogenous leukemia in mice by the P210bcr/abl gene of the Philadelphia chromosome. Science. 1990;247:824-830.
34. Elefanty AG, Hariharan IK, Cory S. bcr-abl, the hallmark of chronic myeloid leukaemia in man,

induces multiple haemopoietic neoplasms in mice. EMBO J. 1990;9:1069-1078.

35. Elefanty AG, Cory S. Hematologic disease induced in BALB/c mice by a bcr-abl retrovirus is influenced by the infection conditions. Mol Cell Biol. 1992;12:1755-1763.
36. Kelliher MA, McLaughlin J, Witte ON, Rosenberg N. Induction of a chronic myelogenous leukemia-like syndrome in mice with v-abl and BCR/ABL [published erratum appears in Proc Natl Acad Sci U S A. 1990;87:9072]. Proc Natl Acad Sci U S A. 1990;87:6649-6653.
37. Gishizky ML, Johnson-White J, Witte ON. Efficient transplantation of Bcr-Abl-induced chronic myelogenous leukemia-like syndrome in mice. Proc Natl Acad Sci U S A. 1993;90:3755-3759.
38. Zhang X, Ren R. Bcr-Abl efficiently induces a myeloproliferative disease and production of excess interleukin-3 and granulocyte-macrophage colony-stimulating factor in mice: a novel model for chronic myelogenous leukemia. Blood. 1998; 92:3829-3840.
39. Pear WS, Miller JP, Xu L, et al. Efficient and rapid induction of a chronic myelogenous leukemia-like myeloproliferative disease in mice receiving P210 bcr/abl-transduced bone marrow. Blood. 1998;92: 3780-3792.
40. Li S, Ilaria RL, Million RP, Daley GQ, Van Etten RA. The P190, P210, and P230 forms of the BCR/ABL oncogene induce a similar chronic myeloid leukemia-like syndrome in mice but have different lymphoid leukemogenic activity. J Exp Med. 1999;189:1399-1412.
41. Gross AW, Zhang X, Ren R. Bcr-Abl with an SH3 deletion retains the ability to induce a myeloproliferative disease in mice, yet c-Abl activated by an SH3 deletion induces only lymphoid malignancy. Mol Cell Biol. 1999;19:6918-6928.
42. Pear WS, Nolan GP, Scott ML, Baltimore D. Production of high-titer helper-free retroviruses by transient transfection. Proc Natl Acad Sci U S A. 1993;90:8392-8396.
43. Ren R, Ye Z, Baltimore D. Abl protein-tyrosine kinase selects the Crk adapter as a substrate using SH3-binding sites. Genes Dev. 1994;8:783-795.
44. Alexandropoulos K, Cheng G, Baltimore D. Proline-rich sequences that bind to Src homology 3 domains with individual specificities. Proc Natl Acad Sci U S A. 1995;92:3110-3114.
45. Alexandropoulos K, Baltimore D. Coordinate activation of c-Src by SH3- and SH2-binding sites on a novel p130Cas-related protein, Sin. Genes Dev. 1996;10:1341-1355.
46. Mayer BJ, Jackson PK, Van Etten RA, Baltimore D. Point mutations in the *abl* SH2 domain coordinately impair phosphotyrosine binding in vitro and transforming activity in vivo. Mol Cell Biol. 1992; 12:609-618.
47. Kelliher MA, McLaughlin J, Witte ON, Rosenberg N. Induction of a chronic myelogenous leukemia-like syndrome in mice with v-abl and BCR/ABL. Proc Natl Acad Sci U S A. 1990;87:6649-6653.
48. Heisterkamp N, Jenster G, ten Hoeve J, Zovich D, Pattengale PK, Groffen J. Acute leukemia in bcr/abl transgenic mice. Nature. 1990;344:251-253.
49. Honda H, Fujii T, Takatoku M, et al. Expression of p210bcr-abl by metallothionein promoter induced T-cell leukemia in transgenic mice. Blood. 1995; 85:2853-2861.
50. Honda H, Oda H, Suzuki T, et al. Development of acute lymphoblastic leukemia and myeloproliferative disorder in transgenic mice expressing p210bcr/abl: a novel transgenic model for human Ph1-positive leukemias. Blood. 1998;91:2067-2075.
51. Voncken JW, Kaartinen V, Pattengale PK, Germeraad WT, Groffen J, Heisterkamp N. BCR/ABL P210 and P190 cause distinct leukemia in transgenic mice. Blood. 1995;86:4603-4611.
52. Hariharan IK, Adams JM, Cory S. bcr-abl oncogene renders myeloid cell line factor independent: potential autocrine mechanism in chronic myeloid leukemia. Oncogene Res. 1988;3:387-399.
53. Sirard C, Laneuville P, Dick JE. Expression of bacr-abl abrogates factor-dependent growth of human hematopoietic M07E cells by an autocrine mechanism. Blood. 1994;83:1575-1585.
54. Anderson S, Mladenovic J. The Bcr-Abl oncogene requires both kinase activity and src-homology 2 domain to induce cytokine secretion. Blood. 1996;87:238-244.
55. el-Ahmady O, Mansour M, Kamel H, Baker A. Granulocyte-macrophage colony stimulating factor and interleukin-6 enhanced white blood cell synthesis of leukotrienes in chronic myelogenous leukemia. Anticancer Res. 1997;17:3179-3182.
56. Jonuleit T, Peschel C, Schwab R, et al. Bcr-Abl kinase promotes cell cycle entry of primary myeloid CML cells in the absence of growth factors. Br J Haematol. 1998;100:295-303.
57. Lajmanovich A, Berthier R, Schweitzer A, Leger J, Hollard D. Constitutive expression of GM-CSF mRNA by CML blast cells is correlated with endogenous megakaryocytic colony formation. Leukemia. 1993;7:1211-1218.
58. Jiang X, Lopez A, Holyoake T, Eaves A, Eaves C. Autocrine production and action of IL-3 and granulocyte colony-stimulating factor in chronic myeloid leukemia. Proc Natl Acad Sci U S A. 1999;96:12804-12809.
59. Nosaka T, Kawashima T, Misawa K, Ikuta K, Mui AL, Kitamura T. STAT5 as a molecular regulator of proliferation, differentiation and apoptosis in hematopoietic cells. EMBO J. 1999;18:4754-4765.
60. Kieslinger M, Woldman I, Moriggl R, et al. Antiapoptotic activity of stat5 required during terminal stages of myeloid differentiation. Genes Dev. 2000;14:232-244.
61. Socolovsky M, Fallon AE, Wang S, Brugnara C, Lodish HF. Fetal anemia and apoptosis of red cell progenitors in Stat5a-/-5b-/- mice: a direct role for Stat5 in Bcl-X(L) induction. Cell. 1999;98:181-191.
62. de Groot RP, Raaijmakers JA, Lammers JW, Jove R, Koenderman L. STAT5 activation by BCR-Abl contributes to transformation of K562 leukemia cells. Blood. 1999;94:1108-1112.
63. Nieborowska-Skorska M, Wasik MA, Slupianek A, et al. Signal transducer and activator of transcription (STAT)5 activation by BCR/ABL is dependent on intact Src homology (SH)3 and SH2 domains of BCR/ABL and is required for leukemogenesis. J Exp Med. 1999;189:1229-1242.
64. Sillaber C, Gesbert F, Frank DA, Sattler M, Griffin JD. STAT5 activation contributes to growth and viability in Bcr/Abl-transformed cells. Blood. 2000; 95:2118-2125.
65. Ghaffari S, Wu H, Gerlach M, Han Y, Lodish HF, Daley GQ. BCR-ABL and v-SRC tyrosine kinase oncoproteins support normal erythroid development in erythropoietin receptor-deficient progenitor cells. Proc Natl Acad Sci U S A. 1999;96: 13186-13190.
66. Tomasson MH, Sternberg DW, Williams IR, et al. Fatal myeloproliferation, induced in mice by TEL/PDGFbetaR expression, depends on PDGFbetaR tyrosines 579/581 [see comments]. J Clin Invest. 2000;105:423-432.